Applied Surface Science 678 (2024) 161120

Contents lists available at ScienceDirect

Applied Surface Science

journal homepage: www.elsevier.com/locate/apsusc

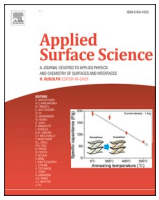

Full Length Article

Dry cleaning of InSb surfaces by hydrogen molecule exposure in ultrahigh vacuum

Zahra Jahanshah Rad, Mikko Miettinen, Marko Punkkinen, Pekka Laukkanen *, Kalevi Kokko

Department of Physics and Astronomy, University of Turku, FI-20014 Turku, Finland

ARTICLE INFO

Keywords:
Surface cleaning
Dry cleaning
Reconstruction
LEED
XPS

ABSTRACT

Cleaning semiconductor surfaces by atomic hydrogen or hydrogen plasma has gained significant interest because such a dry-cleaning method enables to reduce consumption of chemicals and pure water, and to treat challenging surfaces of three-dimensional semiconductor nanostructures. We have studied effects of mere H_2 molecule exposures on (111)B and (110) surfaces of InSb with native oxides in an ultrahigh-vacuum (UHV) chamber. Without any hydrogen cracking, exposure of native-oxide covered InSb(111)B, heated simultaneously at 350 °C, to H_2 with a partial pressure of $5\bullet10^{-5}$ mbar decreases amount of surface oxides and carbon, according to x-ray photoelectron spectroscopy, and provides (2×2) low-energy electron diffraction (LEED) pattern. Scanning tunneling microscopy indicates that this InSb(111)B(2×2) surface contains still extra Sb. When the InSb temperature increases to 400 °C during the H_2 exposure, LEED changes to (3×3) pattern, which is known to arise from a less Sb-rich surface compared to InSb(111)B(2×2). When InSb(111)B(3×3) is exposed to H_2 at the lowered temperature of 300 °C, LEED changes back to (2×2), which is discussed to arise from that InSb(111)B (3×3) contains still oxygen. Experiments for InSb(110) support that the found H_2 exposure effects apply to different crystal faces of InSb.

1. Introduction

Cleaning of semiconductor surfaces is sometimes described as a solved problem in semiconductor technology. However, this crucial step in device manufacturing processes is also developed continuously toward solutions which decrease or constrain the consumption of energy, chemicals, and water in cleaning steps (e.g. Refs. [1–10]). It is worth noting that semiconductor surface cleaning is typically performed several times at different stages of a device manufacturing process. It might be surprising that there is no clear definition for a clean surface; what kind of properties it should have. For example, surface scientists typically expect that a clean semiconductor surface is also well crystalline or ordered, but in general, a clean surface is not necessarily crystalline. In fact, many cleaned surfaces have still a disordered or amorphous atomic structure, although most surface impurities have been removed, because engineering of a well-crystalline surface is difficult and usually requires use of ultraclean ultrahigh vacuum (UHV) environment. The cleaning is here defined to have two effects: to decrease an amount of impurities and to increase a crystalline degree of a surface.

For several decades, the wet chemical treatments have provided a simple and scalable approach to clean various semiconductor surfaces in industry. Dry-cleaning methods have also become more and more relevant to semiconductor technology because the wet chemistry does not work properly for all three-dimensionally structured nanoscale features, and because the consumption of chemicals and pure water is attempted to constrain [6–10]. Furthermore, at some device processing stages (e.g. before metal film deposition), it is useful to clean a surface just before the next processing step *in-situ* manner without exposing the cleaned surface to different environmental conditions.

These challenges in manufacturing semiconductor devices have also motivated surface-science studies. The cleaning of semiconductor surfaces by atomic hydrogen or hydrogen plasma is one of the most investigated dry-cleaning methods (e.g. [11–28]). A hydrogen source is often connected to a UHV chamber, which enables also *in-situ* surface-sensitive measurements such as low-energy electron diffraction (LEED) and x-ray photoelectron spectroscopy (XPS) without the sample transfer to another instrument. LEED provides quickly information about crystalline quality and lattice of a cleaned surface, while XPS is helpful to understand the amount of surface impurities like oxygen and carbon

* Corresponding author.
E-mail address: pekka.laukkanen@utu.fi (P. Laukkanen).

https://doi.org/10.1016/j.apsusc.2024.161120
Received 17 April 2024; Received in revised form 18 August 2024; Accepted 28 August 2024
Available online 30 August 2024

after cleaning. Furthermore, a proper H_2 pre-bake of Si substrates at elevated temperatures (>1000 °C) before chemical vapor deposition of thin films has provided high-quality crystalline Si surfaces with hydrogen passivation [29].

In this work, we have studied if a molecular H_2 exposure provides a cleaning effect at lowered temperatures (≤400 °C) for InSb surfaces. We have used a UHV multi-chamber to perform controlled H_2 exposures and *in-situ* characterization with LEED and XPS for (111)B and (110) surfaces of InSb crystals.

2. Experiments

InSb(111)B and (110) pieces of approximately 5 mm × 10 mm were cut from 2 inch wafers which were slightly n-type, Te-doped ~ 10^{15} cm^{-3}. InSb piece was mounted on Omicron holder where InSb is heated indirect way through W-wire filament beneath the sample holder. After blowing surfaces by nitrogen gas, InSb was loaded in a UHV chamber without any pre-treatment. Background pressure was ~ 10^{-8} mbar range in a preparation chamber where InSb was heated and exposed to H_2. Background pressure was ~ 10^{-10} mbar in an analysis chamber where InSb was *in-situ* characterized by LEED and non-monochromatized XPS (Mg Kα). No electron gun or carbon charging correction was used here in XPS experiments. Pass energy was 40 eV, and number of XPS scans was 5–10 for individual core-level peaks and two for larger survey spectra. XPS spectra were aligned by placing Sb $3d_{5/2}$ peaks from InSb bulk at binding energy (BE) of 528 eV, which provided consistently In $3d_{5/2}$ binding energy of 444 eV. The BE scale was not calibrated in detail with Fermi edge of a metal control sample in this work. XPS energy resolution is limited to near 1 eV due to a non-monochromatized x-ray source. Despite of these limitations in the used XPS instrument, the presented XPS analysis is valid. Sb 3d and In 3d spectra were fitted by using Gaussian shape peaks and Shirley background removal. Scanning tunneling microscopy (Omicron Scala) was also used for some surfaces in the constant current mode at room temperature.

After loading into the UHV preparation chamber, InSb pieces were exposed to H_2 background gas with a partial pressure about $5•10^{-5}$ mbar, and then the temperature of InSb was increased under H_2 exposure. Pure H_2 gas was fed via a leak valve into the preparation chamber pumped by turbo at the same time. Sample distance from the valve varied between 10–70 cm approximately, and according to our observations, sample orientation and distance in relation to the H_2 leak valve did not affect the presented results. Exposure time started from switching on the W-wire filament heater. The heating and H_2 valve were turned off simultaneously. Then it took approximately 5 min to transfer the sample into the analysis chamber for LEED and XPS measurements. During this transfer, some re-adsorption of molecules on the surface occurred probably. On the other hand, an exposure of the cleaned surface to LEED electrons and x-ray photons might remove some re-adsrobed molecules. The InSb temperature was measured by infrared pyrometer.

3. Results and discussion

Fig. 1 shows Sb 3d core-level spectra measured before and after H_2 exposures of InSb(111)B at 350 °C. The O 1 s emission is partially overlapping with Sb 3d. The Sb 3d + O 1 s spectra in Fig. 1 show that amount of oxidized Sb decreases on InSb(111)B significantly due to the H_2 exposure at 350 °C for 30 min (i.e. after exposure of $9·10^4$ Langmuir). After two cycles of the 30-min exposure (i.e. total exposure of $18·10^4$ L), Sb-oxide induced peaks disappeared in XPS. In contrast, In 3d spectra in Fig. 2 do not change visually so much although the peaks narrow slightly due to the H_2 exposures at 350 °C. A spectral fitting in Fig. 2 supports the peak narrowing. Because the O 1 s intensity decreased significantly (Fig. 1), amount of In oxides should decrease also, expecting that the native oxide included both Sb and In oxides, even if the used energy

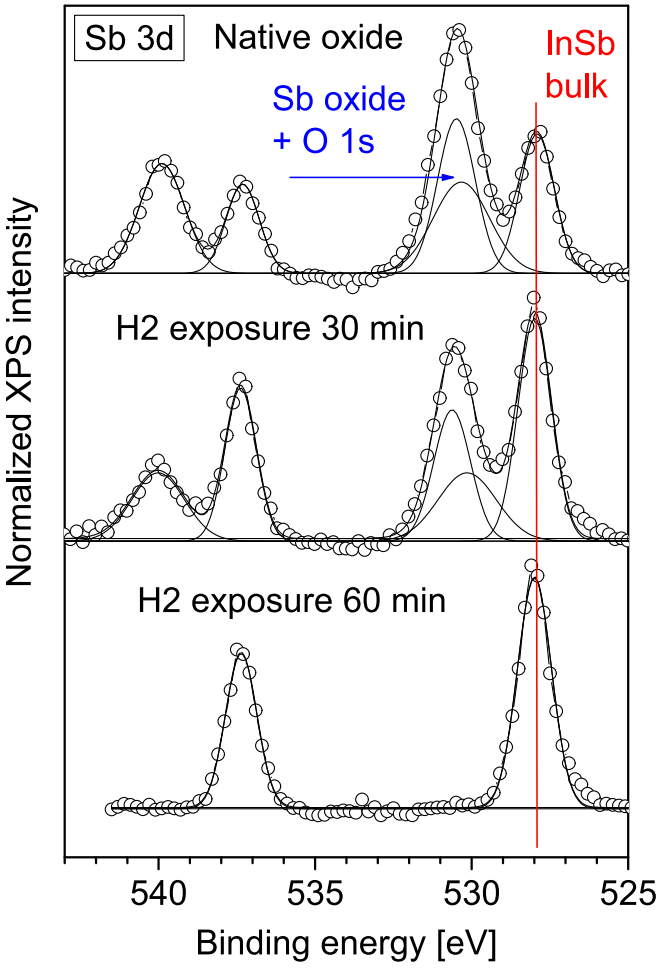

Fig. 1. Sb 3d core-level spectra measured from InSb(111)B before (top spectrum) and after hydrogen treatments (middle and bottom spectra). Temperature of InSb(111)B was 350 °C during H_2 exposures of $5•10^{-5}$ mbar. Emission components of oxidized Sb and O 1s decreased with H_2 exposures. After 30-min H_2 treatment (middle spectrum, exposure of $9·10^4$ Langmuir), the second similar 30-min exposure was done (bottom panel, total exposure of $18·10^4$ Langmuir). The peak intensities were normalized to one.

resolution of XPS did not reveal clear spectral changes in In 3d.

Future synchrotron-radiation XPS measurements hopefully clarify changes in the bonding environment of In atoms induced by H_2 exposures. Previous high-resolution synchrotron-radiation XPS measurements have revealed that an InGaAs surface still includes oxygen atoms bonded particularly to In and Ga after atomic hydrogen treatments [22]. Besides the energy resolution, it is relevant to consider a detectable atom density because it is difficult to resolve the atomic densities lower than $1•10^{12}$ cm^{-2} at a solid surface by XPS, while the defect-induced electron-level density of $1•10^{12}$ cm^{-2} in the band gap causes already significant degradation in device operation. Moreover, the oxidation-induced core-level shifts in the In and Ga spectra are more challenging to interpret than those in the group-V spectra because the presence of oxygen atoms at III-V surfaces can cause also core-level shifts to the low binding-energy side from the bulk peak in the group-III spectra [30–32]. Thus, by no means, we are here able to conclude that all oxygen atoms have been removed from the studied InSb(111)B surface. It means that the studied surfaces can also include water molecules forming in the hydrogen treatment. However, the amount of native oxides clearly decreased when InSb(111)B was treated with the H_2 exposure at 350 °C. Amount of surface carbon also decreased due to the H_2 exposures at 350 °C because C 1s peak disappeared within the XPS resolution, as shown in Fig. 3.

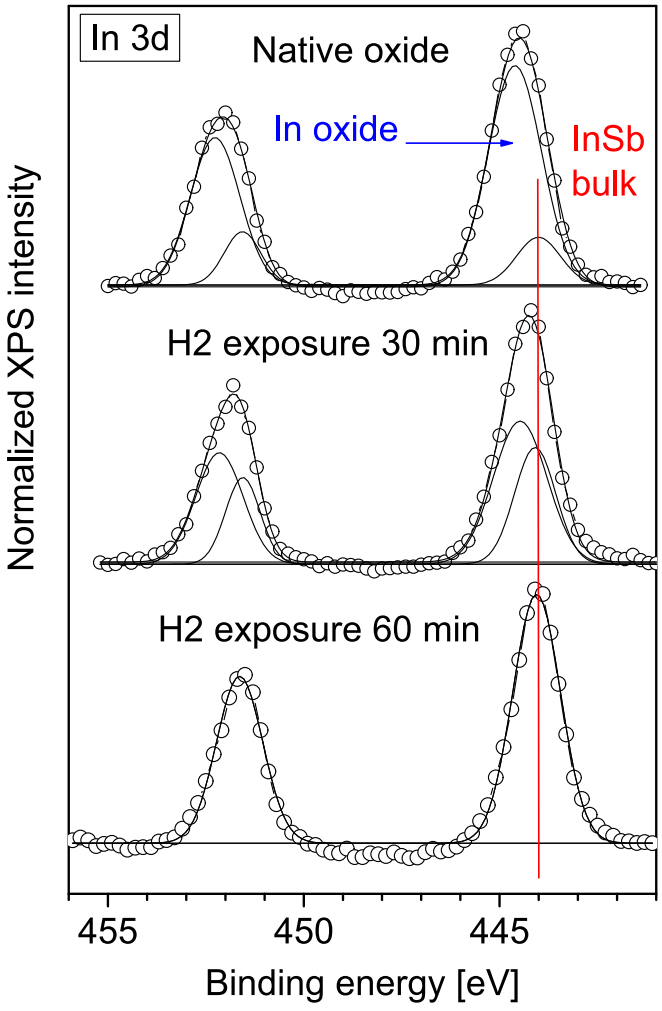

Fig. 2. In 3d core-level spectra measured before and after hydrogen treatments. Temperature of InSb(111)B was 350 °C during H_2 exposure of $5 \bullet 10^{-5}$ mbar. 30-min treatment (middle) means $9 \cdot 10^4$ L exposure of H_2, and 60-min treatment (bottom) means $9 \cdot 10^4$ L+$9 \cdot 10^4$ L exposures. Resolution of used XPS instrument was not high enough to observe clear changes in the spectral shape, although the peaks narrowed slightly with the H_2 exposure. Fitting was done to elucidate the peak narrowing. The peak intensities were normalized to one.

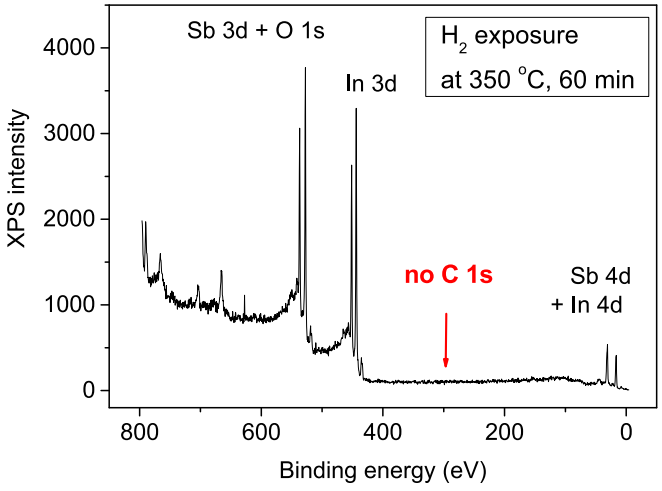

Fig. 3. XPS survey spectrum showed that amount of carbon impurities decreased below XPS resolution after the H_2 cleaning with $9 \cdot 10^4$ L+$9 \cdot 10^4$ L exposure.

LEED observations are consistent with these XPS results. Fig. 4 shows two LEED patterns after the H_2 exposures at two different temperatures 350 °C and 400 °C. LEED showed (2×2) pattern after exposing InSb (111)B to H_2 at 350 °C two times (i.e. 30 min + 30 min → $18 \cdot 10^4$ L). After the first 30-min exposure at 350 °C, (2×2) pattern was visible but weaker. Increasing the InSb temperature during the H_2 exposure to 400 °C changed LEED to (3×3) pattern. The InSb(111)B(3×3) surface is known to include less Sb than InSb(111)B(2×2) [33]. STM measurements (Fig. 5) suggested that the InSb(111)B surface, which showed (2×2) LEED, included also extra Sb clusters or/and SbO_x with lower oxidation state than for those causing the separate Sb-oxide XPS peaks in Fig. 1. It is then reasonable that the exposure at the increased temperature of 400 °C caused the less Sb-rich InSb(111)B(3×3) surface.

It is interesting that re-exposing the InSb(111)B(3×3) surface to H_2 at the lowered temperature of 300 °C changed LEED back to (2×2). This could be understood if the InSb(111)B(3×3) surface contained still oxygen of which amount decreased by the extra H_2 exposure at 300 °C. Such interpretation is consistent with the previous observations for InGaAs that it is difficult to remove all oxygen atoms [22]. Furthermore, the previous controlled oxidation studies of InSb(111)B have shown that the surface with a high crystalline degree can still include oxygen atoms; i.e. crystalline oxygen-containing InSb(111)B(3×3)-O and (2×2)-O can form [33].

The InSb temperature of 350 °C clearly activated the H_2 cleaning effect to remove the native oxides and to induce the (2×2) reconstruction, as shown above. However, exposing the native-oxide covered InSb (111)B to H_2 at 300 °C did not (i) provide a visible LEED pattern and (ii) decrease amount of native oxides much after two 30-min cycles (i.e. $18 \cdot 10^4$ L). Mere heating of the native-oxide covered InSb crystals in UHV, without H_2,, was tested for comparison. Neither 350 °C nor 400 °C heating in UHV resulted in the (2×2) or (3×3) reconstruction in LEED for InSb(111)B. Only (1×1) LEED was observed after heating InSb(111)B in UHV at 400 °C, indicating a disordered surface structure although most surface oxides were removed.

Observations from native-oxide covered InSb(110) surfaces are consistent with the above results. Fig. 6 shows that the amount of native oxides decreases much on InSb(110) during the mere UHV heating at 400 °C without H_2. However, the UHV heating at 350 °C did not provide the same oxide removal. Including the H_2 exposure at 350 °C enhanced the removal of native oxides from InSb(110). Fig. 7 shows LEED from InSb(110) after the UHV heating at 400 °C, which is the (1×1) pattern. Here it is worth noting that clean III-V(110) surfaces do not typically reconstruct, in contrast to the (100) and (111) faces. In other words, (1×1) LEED pattern from III-V(110) can be a sign of well-ordered, crystalline surfaces. Fig. 7 however shows that (1×1) LEED is sharpened when the UHV heated InSb(110)(1×1) surface is further exposed to H_2 exposure at 300 °C. Such a low-temperature effect agrees with the above described reconstruction change of (3×3) to (2×2) on InSb(111) after H_2 exposure at 300 °C. Therefore, although the H_2 exposure at 300 °C does not remove native oxides effectively, it can polish the surfaces, from which most oxides are removed beforehand, increasing their crystalline degree.

It might be useful to combine the atomic hydrogen or hydrogen plasma with the molecular hydrogen exposures in optimizing the hydrogen-based dry-cleaning procedure. For example, it might be interesting to test removing most surface oxides first by the atomic hydrogen or plasma, and then using molecular hydrogen to finalize the cleaning. A gentle H_2 exposure can be expected to reduce crystal damages and even to increase a long-range crystalline order at a cleaned surface, which can be further expected to reduce a density of point defects at surfaces, because a crystalline material includes less point defects than the disordered one. We still note that a reduced UHV background pressure lower than that used in this work (~10^{-8} mbar) is expected to enhance the cleaning effect.

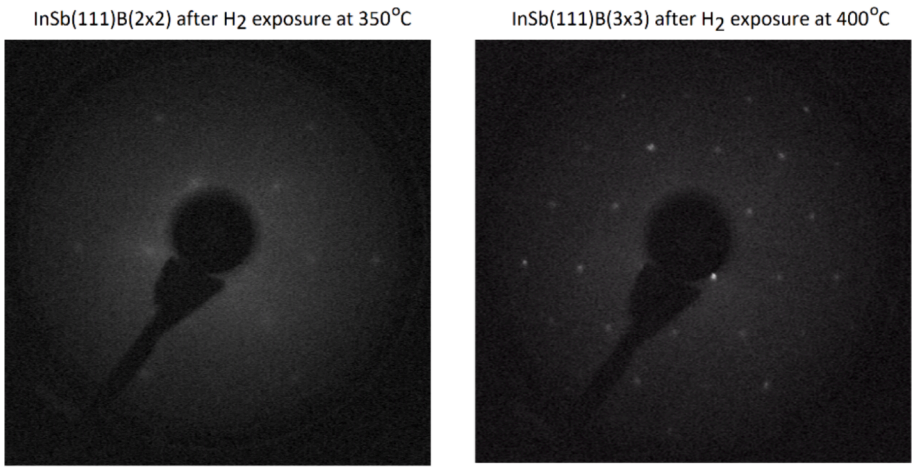

Fig. 4. LEED diffraction pattern of (2×2) reconstruction appeared after H_2 exposure of $9{\cdot}10^4$ L+$9{\cdot}10^4$ L at 350 °C. When the temperature of this same InSb(111)B surface increased at 400 °C under H_2 exposure $9{\cdot}10^4$ L (i.e. totally $9{\cdot}10^4$ L+$9{\cdot}10^4$ L+$9{\cdot}10^4$ L), LEED changed to (3×3).

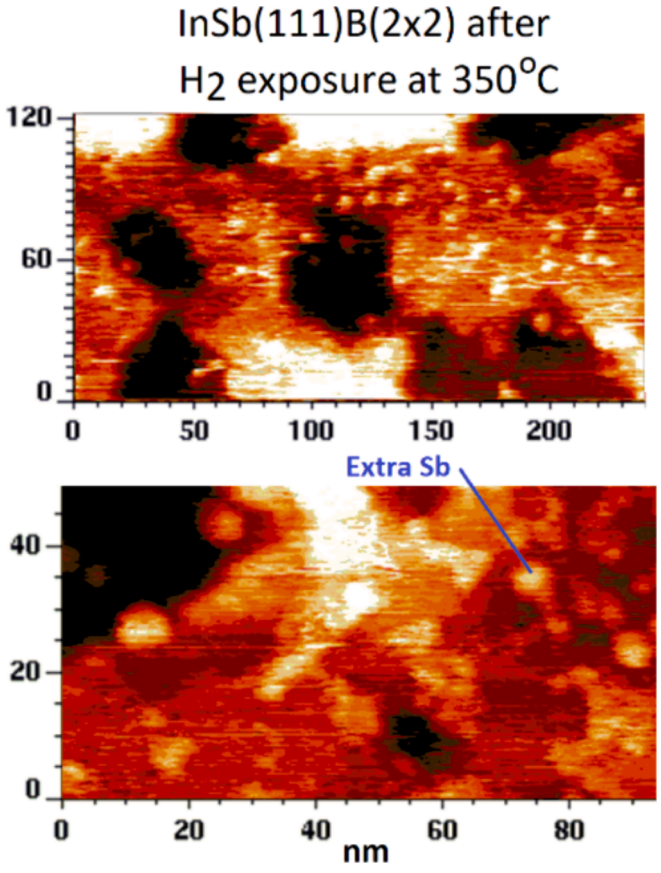

Fig. 5. STM showed formation of two-dimensional islands after the H_2 exposure at 350 °C for 60 min (i.e. $9{\cdot}10^4$ L+$9{\cdot}10^4$ L exposures). On top of the islands, there are cluster features which are interpreted as extra Sb or SbO_x.

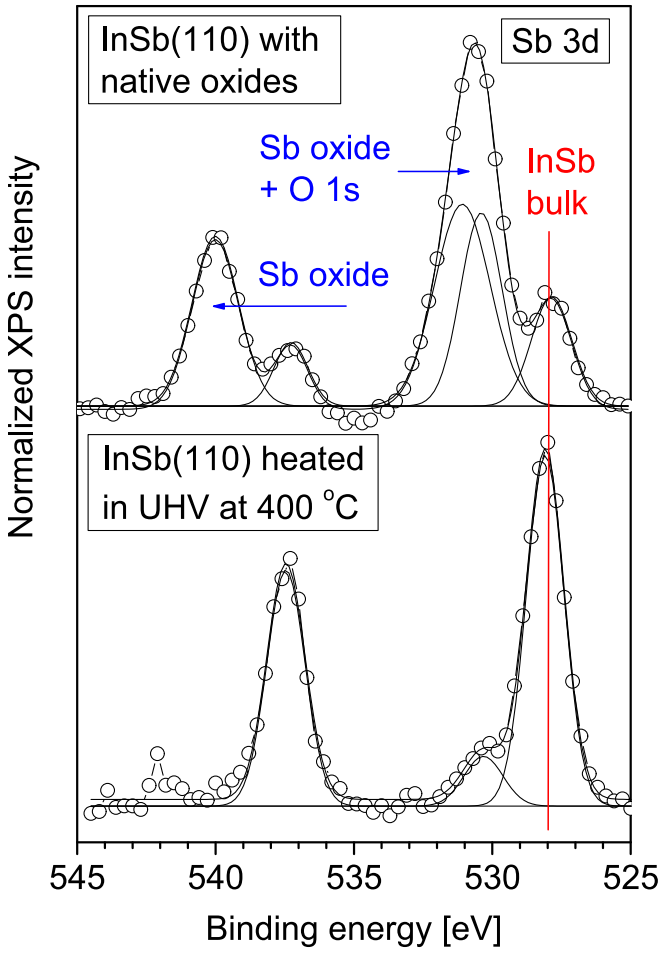

Fig. 6. XPS spectra from native-oxide covered InSb(110) surface before and after heating (400°C) in UHV without hydrogen showed that the 400°C heating removed most native oxides. The peak intensities were normalized to one.

4. Conclusions

With XPS and LEED measurements, we found that the H_2 exposure at 350–400 °C provided a dry-cleaning effect for (111)B and (110) surfaces of InSb crystals. XPS showed that the amount of Sb and In oxides as well as carbon decreased after exposing the native-oxide covered InSb surfaces to H_2 when the InSb temperature was 350 °C. Concomitantly the LEED pattern became visible: namely (2×2) for InSb(111)B and (1×1) for InSb(110). LEED changed to (3×3) when the InSb(111)B(2×2) surface was further exposed to H_2 at 400 °C, indicating that Sb amount decreased at the surface. When this InSb(111)B(3×3) was again exposed to H_2 at 300 °C, LEED changed back to (2×2), which was explained by removal of In oxides from oxygen-containing InSb(111)B(3×3)-O, even if no change was observed in XPS.

The mere UHV heating at 400 °C without H_2 removed most native

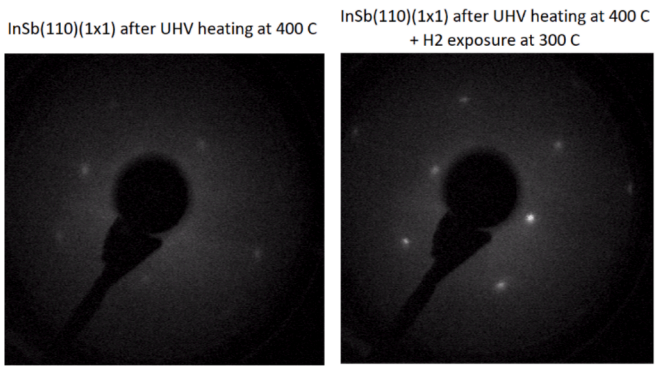

Fig. 7. Left: LEED pattern of (1×1) was visible after heating native-oxide covered InSb(110) in UHV at 400°C for 30 min without H_2. The (1×1) unit cell is rectangular and is tilted here due to sample tilting on the holder. Right: When this UHV-heated InSb(110)(1×1) surface was further exposed to H_2 at 300 °C for 30 min, i.e. $9{\cdot}10^4$ L exposure, (1×1) LEED became sharper indicating that long-range crystalline degree increased at the surface.

oxides and carbon contamination, according to XPS, but including the H_2 exposures in the cleaning process increased crystalline order at the InSb surfaces. Namely, UHV heating at 400 °C without H_2 did not cause any reconstruction on InSb(111)B, and (1×1) LEED from InSb(110) sharpened with using H_2. Thus, the H_2 exposure of a properly heated semiconductor surface could be a useful method to optimize cleanliness and crystal structure of semiconductor surfaces during device manufacturing processes.

CRediT authorship contribution statement

Zahra Jahanshah Rad: Writing – review & editing, Validation, Methodology, Investigation. **Mikko Miettinen:** Writing – review & editing, Validation, Methodology, Investigation. **Marko Punkkinen:** Writing – review & editing, Supervision. **Pekka Laukkanen:** Writing – original draft, Supervision. **Kalevi Kokko:** Writing – review & editing, Supervision.

Declaration of competing interest

The authors declare that they have no known competing financial interests or personal relationships that could have appeared to influence the work reported in this paper.

Data availability

Data will be made available on request.

References

[1] Proceedings of the fourth international symposium on cleaning technology in semiconductor device manufacturing. Edited by R. E. Novak, J. Ruzyllo, Electrochemical Society Proceedings 95-20 (1996).
[2] T. Takahagi, S. Shingubara, H. Sakaue, Wet preparation of defect-free hydrogen-terminated silicon wafer surface and its characterization in atomic-scale. (UCPSS 2000), Sol. State Phenom. 76-77 (2001) 105.
[3] F. De Smedt, S. De Gendt, M. Claes, M.M. Heyns, H. Vankerckhoven, C. Vinckier, The increasing importance of the use of ozone in the microelectronics industry, Ozone Sci. Eng. 24 (2002) 379.
[4] B. Onsia, M. Caymax, T. Conard, S. De Gendt, F. De Smedt, A. Delabie, C. Gottschalk, M. Green, M. Heyns, S. Lin, P. Mertens, W. Tsai, C. Vinckier, On the application of a thin ozone based wet chemical oxide as an interface for ALD high-k deposition, Diff, Defect Data Pt.b: Sol. State Phenom. (2005).
[5] H. Kato, T. Taoka, S. Nishikata, G. Sazaki, T. Yamada, R. Czajka, A. Wawro, K. Nakajima, A. Kasuya, S. Suto, Preparation of an ultraclean and atomically controlled hydrogen-terminated Si(111)-(1x1) surface revealed by high resolution electron energy loss spectroscopy, atomic force microscopy, and scanning tunneling microscopy: aqueous NH4F etching process of Si(111), Jpn. J. Appl. Phys. 46 (2007) 5701.
[6] D.-H. Im, K.-S. Lee, Y. Kang, M. Jeong, K.W. Park, S.-G. Lee, M. Jin-Won, Y. Kim, B. Kim, K.-V. Im, H. Lim, J.Y. Lee, Interfacial layer control by dry cleaning technology for polycrystalline and single crystalline silicon growth, J. Nanoscience Nanotechn. 16 (2016) 4906.
[7] J.W. Park, M.G. Chae, D.S. Kim, W.O. Lee, H.D. Song, C. Choi, G.Y. Yeom, In situ dry cleaning of Si wafer using OF2/NH3 remote plasma with low global warming potential, J. Phys. D Appl. Phys. 51 (2018) 445201.
[8] C. Ahles, J. Choi, R. Hung, N. Kim, S. Nemani, A. Kummel, Selective etching of native silicon oxide in preference to silicon oxide and silicon, International Symposium on VLSI Technology, Systems and Application (2019) 978-1-7281-0942-8/19.
[9] M. Ruberti, The chip manufacturing industry: environmental impacts and eco-efficiency analysis, Sci. Total Environ. 858 (2023) 159873.
[10] E. Gallagher, P. Bezard, L. Boakes, A. Firrincieli, C. Rolin, L.-Å. Ragnarsson, Sustainable semiconductor manufacturing: lessons for lithography and etch, SPIE Proceed. 12499 (2023).
[11] I. Suemune, Y. Kunitsugu, Y. Kan, M. Yamanishi, Incidence angle effect of a hydrogen plasma beam for the cleaning of semiconductor surfaces, Appl. Phys. Lett. 55 (1989) 760.
[12] Y.J. Chun, T. Sugaya, Y. Okada, M. Kawabe, Low temperature surface cleaning of InP by irradiation of atomic hydrogen, Jpn. J. Appl. Phys. 32 (1993) L287.
[13] G.R. Bell, N.S. Kaijaks, R.J. Dixon, C.F. McConville, Atomic hydrogen cleaning of polar III–V semiconductor surfaces, Surf. Sci. 401 (1998) 125.
[14] L. Haworth, J. Lu, D.I. Westwood, J.E. MacDonald, Atomic hydrogen cleaning, nitriding and annealing InSb (100), Appl. Surf. Sci. 166 (2000) 253.
[15] K. Asai, K. Komachi, K. Kamei, H. Katahama, Hydrogen plasma irradiation and postannealing effects on crystalline quality at vicinal Si 100 surface, Appl. Surf. Sci. 153 (2000) 134.
[16] Ch. Förster, F. Schnabel, P. Weih, Th. Stauden, O. Ambacher, J. Pezoldt, In situ spectroscopic ellipsometry of hydrogen-argon plasma cleaned silicon surfaces, Thin Solid Films 455–456 (2004) 695.
[17] A. Khatiri, J.M. Ripalda, T.J. Krzyzewski, G.R. Bell, C.F. McConville, T.S. Jones, Atomic hydrogen cleaning of GaAs(001): a scanning tunnelling microscopy study, Surf. Sci. 548 (2004) L1.
[18] A. Aßmuth, T. Stimpel-Lindner, O. Senftleben, A. Bayerstadler, T. Sulima, H. Baumgärtner, I. Eisele, The role of atomic hydrogen in pre-epitaxial silicon substrate cleaning, Appl. Surf. Sci. 253 (2007) 8389.
[19] W. Melitz, J. Shen, T. Kent, R. Droopad, P. Hurley, A.C. Kummel, Atomic imaging of atomic H cleaning of InGAs and InP for ALD, ECS Trans. 35 (2011) 175.
[20] J. Park, J.G. Cruz, B. Zheng, J. Gelatos, M. Narasimhan, P.K. Narwankar, A novel approach to clean surface for high mobility channel materials with in situ atomic hydrogen clean, ECS Trans. 58 (2013) 275.
[21] R.K. Chellappan, Z. Li, G. Hughes, Synchrotron radiation photoemission study of the thermal annealing and atomic hydrogen cleaning of native oxide covered InAs (1 0 0) surfaces, Appl. Surf. Sci. 276 (2013) 609.
[22] B. Brennan, K. Kumarappan, G. Hughes, Atomic hydrogen cleaning of In0.53Ga0.47As studied using synchrotron radiation photoelectron spectroscopy, Phys. Status Sol. RRL 7 (2013) 989.
[23] X. Qin, B. Brennan, H. Dong, J. Kim, C.L. Hinkle, R.M. Wallace, In situ atomic layer deposition study of HfO2 growth on NH4OH and atomic hydrogen treated Al0.25Ga0.75N, J. Appl. Phys. 113 (2013) 244102.
[24] M. Barth, G.B. Rayner Jr., S. McDonnell, R.M. Wallace, B.R. Bennett, R. Engel-Herbert, S. Datta, High quality HfO2/p-GaSb(001) metal-oxide-semiconductor capacitors with 0.8 nm equivalent oxide thickness, Appl. Phys. Lett. 105 (2014) 222103.
[25] T. Kaufman-Osborn, K. Kiantaj, C.-P. Chang, A.C. Kummel, In-situ non-disruptive cleaning of Ge(100) using H2O2(g) and atomic hydrogen, Surf. Sci. 630 (2014) 254.
[26] J.L. Webb, J. Knutsson, M. Hjort, S.G. Ghalamestani, K.A. Dick, R. Timm, A. Mikkelsen, Electrical and surface properties of InAs/InSb nanowires cleaned by atomic hydrogen, NanoLett. 15 (2015) 4865.
[27] Y.-P. Liu, S. Yngman, A. Troian, G. D'Acunto, A. Jönsson, J. Svensson, A. Mikkelsen, L.-E. Wernersson, R. Timm, Hydrogen plasma enhanced oxide removal on GaSb planar and nanowire surfaces, Appl. Surf. Sci. 593 (2022) 153336.
[28] S. Yun, P.-C. Lee, C.-H. Kuo, A.J. Mcleod, Z. Zhang, V. Wang, J. Huang, H. Kashyap, C.H. Winter, A.C. Kummel, Gallium phosphide conformal film growth on in-situ tri-TBP dry-cleaned InGaP/GaAs using atomic hydrogen ALD, Vacuum 220 (2024) 112806.
[29] O. Vatel, S. Verhaverbeke, H. Bender, M. Caymax, F. Chollet, B. Vermeire, P. Mertens, E. André, M. Heyns, Atomic force microscopy and infrared spectroscopy studies of hydrogen baked Si surfaces, Jpn. J. Appl. Phys. 32 (1993) L1489.
[30] J.J.K. Lång, M.P.J. Punkkinen, M. Tuominen, H.-P. Hedman, M. Vähä-Heikkilä, V. Polojärvi, J. Salmi, V.-M. Korpijärvi, K. Schulte, M. Kuzmin, R. Punkkinen, P. Laukkanen, M. Guina, K. Kokko, Unveiling and controlling the electronic structure of oxidized semiconductor surfaces: crystalline oxidized InSb(100)(1×2)-O, Phys. Rev. B 90 (2014) 045312.
[31] M. Tuominen, J. Lång, J. Dahl, M. Kuzmin, M. Yasir, J. Mäkelä, J.R. Osiecki, K. Schulte, M.P.J. Punkkinen, P. Laukkanen, K. Kokko, Oxidized crystalline (3 × 1)-

O surface phases of InAs and InSb studied by high-resolution photoelectron spectroscopy, Appl. Phys.Lett. 106 (2015) 011606.
[32] J. Mäkelä, A. Lahti, M. Tuominen, M. Yasir, M. Kuzmin, P. Laukkanen, K. Kokko, M.P.J. Punkkinen, H. Dong, B. Brennan, R.M. Wallace, Unusual oxidation-induced core-level shifts at the HfO2/InP interface, Sci. Rep. 9 (2019) 1462.
[33] J. Mäkelä, Z. Jahanshah Rad, J.-P. Lehtiö, M. Tuominen, J. Dahl, M. Kuzmin, M.P. J. Punkkinen, P. Laukkanen, K. Kokko, Crystalline oxide phases on InSb(111)B revealed with scanning tunneling microscopy and spectroscopy, Sci. Rep. 8 (2018) 14382.